

Structural Health Monitoring

<http://shm.sagepub.com/>

Identification of a Crack in a Rotor System using a Model-based Wavelet Approach

A. S. Sekhar

Structural Health Monitoring 2003 2: 293

DOI: 10.1177/147592103039917

The online version of this article can be found at:

<http://shm.sagepub.com/content/2/4/293>

Published by:



<http://www.sagepublications.com>

Additional services and information for *Structural Health Monitoring* can be found at:

Email Alerts: <http://shm.sagepub.com/cgi/alerts>

Subscriptions: <http://shm.sagepub.com/subscriptions>

Reprints: <http://www.sagepub.com/journalsReprints.nav>

Permissions: <http://www.sagepub.com/journalsPermissions.nav>

Citations: <http://shm.sagepub.com/content/2/4/293.refs.html>

>> [Version of Record](#) - Dec 1, 2003

[What is This?](#)

Identification of a Crack in a Rotor System Using a Model-based Wavelet Approach

A. S. Sekhar*

*Technische Universität Darmstadt, Institute für Mechanik AG 2,
Hochschulstrasse 1, D - 64289 Darmstadt, Germany*

The dynamics and diagnostics of a cracked rotor have been gaining importance in recent years. Vibration monitoring during start-up or shut-down is as important as during steady-state operations to detect cracks especially for machines such as aircraft engines which start and stop quite frequently and run at high speeds. In the present study, a model-based method is proposed for the on-line identification of cracks in a rotor while it is passing through its flexural critical speed. The fault-induced change of the rotor system is taken into account by equivalent loads in the mathematical model. The equivalent loads are virtual forces and moments acting on the linear undamaged system to generate a dynamic behaviour identical to the measured one of the damaged system. The rotor has been modelled using FEM, while the crack is considered through local flexibility change. The crack has been identified for its depth and location on the shaft for different rotor accelerations. The nature and symptoms of the fault – crack – are further ascertained using the continuous wavelet transform.

Keywords crack · model-based approach · modal expansion · wavelet · transient · FEM

1 Introduction

An important rotor fault, which can lead to catastrophic failure if undetected, is fatigue cracks in the shaft. Vibration behaviour of cracked structures, in particular cracked rotors, has received considerable attention in the last three decades [1–3]. The problem of damage and crack identification in structural components has acquired an important role in recent years. Severe damages in power plants have been reported by Hass [4] and Muszynska [5]. The efforts to successfully detect the crack started way back, the simple hinge model of Gasch [6] to demonstrate the breathing crack is one such. Mayes and Davies [7] based on the energy rate approach developed models to locate the position and size

of a crack. Inagaki et al. [8] have used transfer matrix approach by a step function for the bending moment to model the breathing of crack.

The increasing concern over early crack detection or rotor failures due to the presence of a crack has accelerated the development of non-destructive techniques based on changes of the modal parameters of the system [9]. As summarized by Hamidi et al. [9], several publications have proposed the use of several techniques such as the use of natural frequencies, mode shapes and frequency response functions for the damage detection.

Modern machinery is bound to fulfill increasing demands concerning durability as well as safety requirements. The concepts of a continuous on-line monitoring system with real-time reporting

*E-mail: sekhar@mech.iitkgp.ernet.in
On Humboldt Fellowship to TUD, Darmstadt, Germany
Mechanical Engineering Department, IIT Kharagpur, India

offers the promise of improved knowledge of the condition of a machine and therefore fewer uncertainties in the operating decisions. Edwards et al. [10] have provided a broad review of the state of the art in fault diagnosis techniques, with particular regard to rotating machinery. It has been seen that new model-based fault diagnosis are being developed rapidly in order to meet the demand for increasingly intelligent condition monitoring systems for the maintenance of modern industrial process. On-line condition monitoring strategies will become increasingly commonplace in a greater range of systems.

Seibold and Weinert [11] investigated on the detection techniques based on Extended Kalman filters to detect the position and depth of crack whereby each filter represents a different damage scenario. Recently, Markert et al. [12–14] proposed a model-based method which allows the online identification of malfunctions in rotor systems. They presented the models in which equivalent loads due to the faults such as rubbing and unbalance as virtual forces and moments acting on the linear undamaged system model to generate a dynamic behaviour are identical to the measured one of the damaged system. The identification is then performed by least squares fitting in the time domain. Edwards et al. [15] employed a model-based identification in the frequency domain to identify an unbalance on a test-rig. A more comprehensive approach to identify different types of faults has been reported in [16].

For diagnosing the state of a machine, usually signal-based monitoring systems are used as good tools, although they do not fully utilize the information contained within the vibration data. These approaches to machinery diagnostics are generic rather than machine specific and the interpretation of the data is based on qualitative rather than quantitative information. Contrary to signal-based monitoring systems, model-based diagnostics systems developed in recent years [17,18] utilize all information contained in the continuously recorded vibration signals. These methods work either in the time or in the frequency domain depending on the malfunction type and the operating state for which the vibration data are available. Also it can be used

together with or alternatively to conventional signal-based monitoring systems.

Most of the previous works focussed on detecting rotor cracks by analyzing the steady-state vibrations of a rotor bearing system. Vibration monitoring during start-up or shut-down is as important as during steady-state operation to detect cracks. But research on transient responses of the cracked rotor passing the critical speed has been limited, although some recent works have been reported [19–21]. However, many works used speed-response, time domain signals and/or the traditional signal processing technique such as FFT with modifications to suit the non-stationary vibration signals to detect cracks. The wavelets provide time-scale information of a signal, enabling the extraction of features that vary in time. This property makes “wavelets” an ideal tool and an alternate.

The theory of the orthogonal wavelets and their application to signal analysis have been presented by Newland [22, 23]. An excellent recent review by Staszewski [24] gives various wavelet methodologies for damage detection. In a recent paper [25] the effectiveness of wavelet transforms was shown for crack detection and monitoring in rotors.

In the present study a model-based technique for the crack identification is discussed. Previously, the model-based techniques were employed to identify faults. But to the best of the author’s knowledge, the simulations of crack identification using equivalent loads (virtual loads) in the model-based approach and that to for the transient rotors are not demonstrated in literature. Also in the present paper, the combined approach of model-based using the equivalent loads followed by signal-based approach using continuous wavelet technique (CWT) for a rotor passing the flexural critical speed has been suggested for crack identification.

2 Identification Method

In the present study, model-based identification method [13,14] is used, which is based on the idea that system faults can be represented by virtual loads ΔF that act on the linear undamaged

system model. Equivalent loads are fictitious forces and moments, which generate the same dynamic behaviour as the real non-linear damaged system does. This method enables to maintain linear, so that fast analysis can be carried out to identify faults while the machine is still running.

2.1 Mathematical Description

The vibrations represented by the vector $r_o(t)$ at N degrees of freedom (DOF) of the undamaged rotor system due to the operating load $F_o(t)$ during normal operation are described by the linear equation of motion:

$$M_o \ddot{r}_o(t) + D_o \dot{r}_o(t) + K_o r_o(t) = F_o(t) \quad (1)$$

where M_o , D_o , K_o are mass, damping and stiffness matrices of any complex rotor system, which can include the effects of bearings, foundation and gyroscopic forces etc.

The occurrence of a fault changes the dynamic behaviour of the system; the extent of the change depends on the vector β , which describes the fault parameters like type, magnitude and location etc. of the fault. The fault-induced change in the vibrational behaviour is represented by the additional loads acting on the undamaged system.

$$M_o \ddot{r}(t) + D_o \dot{r}(t) + K_o r(t) = F_o(t) + \Delta F(\beta, t) \quad (2)$$

The residual vibrations induced represent the difference of the previously measured normal vibrations of the undamaged system from vibrations of the currently measured damaged system.

$$\begin{aligned} \Delta r(t) &= r(t) - r_o(t); & \Delta \dot{r}(t) &= \dot{r}(t) - \dot{r}_o(t); \\ \Delta \ddot{r}(t) &= \ddot{r}(t) - \ddot{r}_o(t) \end{aligned} \quad (3)$$

Subtraction of the equations of motion for the undamaged (Equation (1)) from that of the damaged (Equation (2)), and using Equation (3), yields the equation of motion for the residual vibration as given by,

$$M_o \Delta \ddot{r}(t) + D_o \Delta \dot{r}(t) + K_o \Delta r(t) = (\beta, t) \quad (4)$$

The system matrices remain unchanged and the rotor model stays linear. Only the equivalent loads induce the change in the dynamic behaviour of the undamaged linear rotor model. To identify the fault parameters, the difference of the theoretical fault model and the measured equivalent loads will be minimized by a least squares fitting algorithm.

For calculating the fault-induced residual vibrations, measured vibration data for both the undamaged and damaged rotor system have to be available for the same operating and measurement conditions. For example, differences in the rotor speeds, phase and the sampling times have to be taken into account. Different rotor speeds, for instance, are compensated by adjusting the time-scale of the normal vibrations to the time-scale of the currently measured vibrations. Similarly for others, because directly matching data are usually not available, some signal processing has to be done to achieve the same conditions [13,14].

The definition of the additional vibrations during rapid transients is a difficult task. However, for small time steps, during that time duration, the accelerations and the other conditions can be assumed to be identical in real machines.

2.2 Modal Expansion

For calculating the equivalent loads from the mathematical model of the rotor system by Equation (4), measured residual vibrations must be available at all DOF of the model. Since the vibrations are measured only at a few DOF in practice, the vibrations at non-measured DOF must be estimated using the measured vibrations. Therefore, the residual vibrations need to be reconstructed via modal expansion from the directly measured vibrations such as $\Delta \tilde{r}_M(t)$, at the measuring positions. This technique is based on the approximation of the residual vibration by a linear combination of only a few eigenvectors. Simultaneously, a set of equivalent loads representing the malfunctions is calculated from the measured vibration signals using the mathematical model of the undamaged rotor system.

By comparing the equivalent loads reconstructed from the current measurements to the pre-calculated equivalent loads resulting from fault models, the type, amount and location of the current fault can be estimated. The identification method is based on least squares fitting algorithms in the time domain. The quality of the fit is used to find the probability that the identified fault is present.

As explained before, the residual vibrations $\Delta\tilde{r}_M(t)$ are available only for a few DOF of the model. The number M of the measurement locations is much smaller than the number N , the DOF of the model. The data of the non-measurable DOF have to be estimated from the measured signals. The measurable part $\Delta\tilde{r}_M(t)$ of the residual vector is related to the full residual vector $\Delta\tilde{r}(t)$ by the measurement matrix C ,

$$\Delta\tilde{r}_M(t) = C\Delta\tilde{r}(t) \quad (5)$$

The full residual vector can be approximated by a set of mode shapes \hat{r}_k which are put together in the reduced modal matrix

$$\hat{\phi} = [\hat{r}_1, \hat{r}_2, \dots, \hat{r}_k]. \quad (6)$$

Logically, the number K of mode shapes used may not exceed the number M of independently measured vibration signals contained in $\tilde{r}_M(t)$, $K \leq M$. The vector of modal co-ordinates $\Delta q(t)$ is estimated by combining the measurement Equation (5) with modal representation

$$\Delta\tilde{r}(t) = \hat{\phi}\Delta q(t) \quad (7)$$

of the full residual vector and minimising the equation error by the least squares method. Eventually, the full residual vector at all DOF is estimated by

$$\Delta\tilde{r}(t) = \{\hat{\phi}[(C\hat{\phi})^T(C\hat{\phi})]^{-1}[C\hat{\phi}]^T\}\Delta\tilde{r}_M(t) = Q\Delta\tilde{r}_M(t) \quad (8)$$

where the constant matrix Q can be calculated in advance.

2.3 Equivalent Loads

The equivalent load $\Delta\tilde{F}(t)$ characterising the unknown fault is calculated by substituting the residual vibrations of the full vibrational state into Equation (4), together with Equation (8), yielding,

$$\Delta\tilde{F}(t) = M_o Q \Delta\ddot{\tilde{r}}_M(t) + D_o Q \Delta\dot{\tilde{r}}_M(t) + K_o Q \Delta\tilde{r}_M(t) \quad (9)$$

Only simple matrix multiplications and additions have to be carried out, for estimating the equivalent loads from the measured vibration signals. Thus, it is very suitable for on-line identification of crack or any other fault.

2.4 Fault Models

For the model-based fault identification method, each fault has to be represented by a mathematical model describing the relation between the fault parameters β and the equivalent force $\Delta\tilde{F}(t)$. Hence, $\Delta F(\beta, t)$ is a mathematical expression for the time history of the forces acting on the individual DOF of the model. The fault vector β in this case contains the crack depth and location. A detail explanation on crack, the fault considered in this paper is given in a separate section. The basic idea to model a transverse crack in a shaft is to consider the change of the cracked element's stiffness. The changed stiffness of the cracked element is multiplied with the displacement vector $r(t)$ which yields the equivalent force,

$$\Delta F_{cr}(\beta, t) = r(t) \quad (10)$$

2.5 Least Squares Fitting in the Time Domain

For identifying the fault parameters, the equivalent loads from measured vibrations and those from the mathematical model should be compared. If there were no noise and no errors due to modal expansion, the equivalent loads, $\Delta\tilde{F}(t)$ from measured data would match exactly to loads $\Delta F(t)$ of a certain mathematical fault

model. Since the measured signals and their processing are always associated with some noise and inevitable errors, the best fit between the two loads pattern is sought by adjusting the fault parameter fault model β . The least squares algorithm is used in time domain to achieve the best curve fitting. The objective function to be minimized for the measured equivalent forces $\Delta\tilde{F}(t)$ and the theoretical ones (or of a certain mathematical model) $\Delta F_i(\beta_i, t)$, is given as

$$\int \left| \sum_i \Delta F_i(\beta_i, t) - \Delta\tilde{F}(t) \right|^2 dt = \text{Min} \quad (11)$$

The algorithm iterates for the values of fault parameters β_i for all suspected faults taken into account. For example in the present paper, the fault considered is crack. A small amount of crack depth is assumed to start with in the element no.1 and the algorithm is iterated in the program. Then the process is repeated considering crack in the next element and so on for all the elements for the same depth of crack. The process is repeated for different depths by a small increment and preceded to do the iteration, till objective function is satisfied. Thus the crack depth and location can be identified. If more faults are there, fault parameters β_i for all suspected faults shall be taken into account. This eventually leads to identification of the fault type, its position and the extent. The least square technique can be used in the frequency domain as well. Matlab version 6.0 has been used to solve the algorithm. More details of the algorithm can be seen in [13,14].

2.6 Probability Measures

The quality of fit achieved can be used to estimate the probability of the different identified faults. Two probability measures based on correlation functions have been developed and successfully tested in [14]. These are also used here. The first probability measure p_1 , called coherence, is the normalized correlation of the identified equivalent forces $\Delta F_i(\beta_i, t)$ of a particular fault

with the measured equivalent forces $\Delta\tilde{F}(t)$ for lag $\tau=0$,

$$p_1 = \phi_{\Delta F_i, \Delta\tilde{F}}(0) / \sqrt{\phi_{\Delta F_i, \Delta F_i}(0)\phi_{\Delta\tilde{F}(t), \Delta\tilde{F}}(0)} \quad (12)$$

Due to the normalisation by the auto-correlation functions of $\Delta F_i(\beta_i, t)$ and $\Delta\tilde{F}(t)$, the coherence takes values between $-1 \leq p_1 \leq 1$, where $p_1=1$ means that $\Delta F_i(\beta_i, t)$ matches $\Delta\tilde{F}(t)$ perfectly.

The other probability measure p_2 , called the intensity, measures the contribution of the particular fault to the measured total equivalent forces $\Delta F_{\text{ident}} = \sum \Delta F_i$,

$$p_2 = \phi_{\Delta F_i, \Delta F_i}(0) / \phi_{\Delta F_{\text{ident}}, \Delta F_{\text{ident}}}(0). \quad (13)$$

The intensity measures takes values in the interval $0 \leq p_2 \leq 1$, where $p_2=1$ signifies that the identified fault is the only one present in the rotor system. It was reported in [13,14], that both measures p_1 and p_2 should be used simultaneously to evaluate the probability of a fault. Suitable threshold values are $p_1 \geq 10\%$ and $p_2 \geq 20\%$ indicating that specific fault is present in the rotor system [14].

The whole process of identification is shown in the Figure 1. The measured vibration signals $\tilde{r}_M(t)$ are the input and the fault parameters β_i for each fault are the output.

3 System Equation of Motion

The rotor-bearing system is discretized into finite beam elements [26] as shown in Figure 2, together with details of shaft element. The DOF of the model considered are two deflections and two translations at each node with the q_1 to q_8 are the nodal quantities. Even though the figure is shown with crack, all the configuration and details are also valid for uncracked rotor. The equation of motion of the complete rotor system in a fixed co-ordinate system can be written as,

$$[M]\{\ddot{q}\} + [D]\{\dot{q}\} + [K]\{q\} = \{F\} \quad (14)$$

where the mass matrix $[M]$ includes the rotary and translational mass matrices of the shaft,

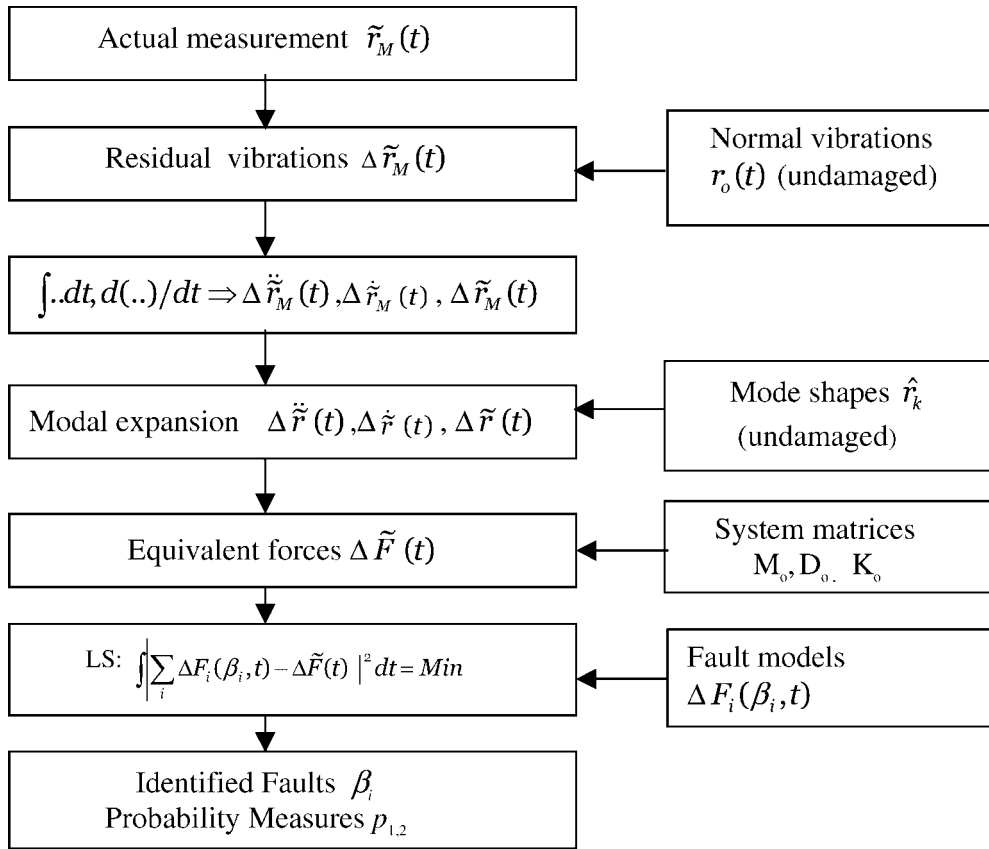


Figure 1 Flow chart of the fault identification method.

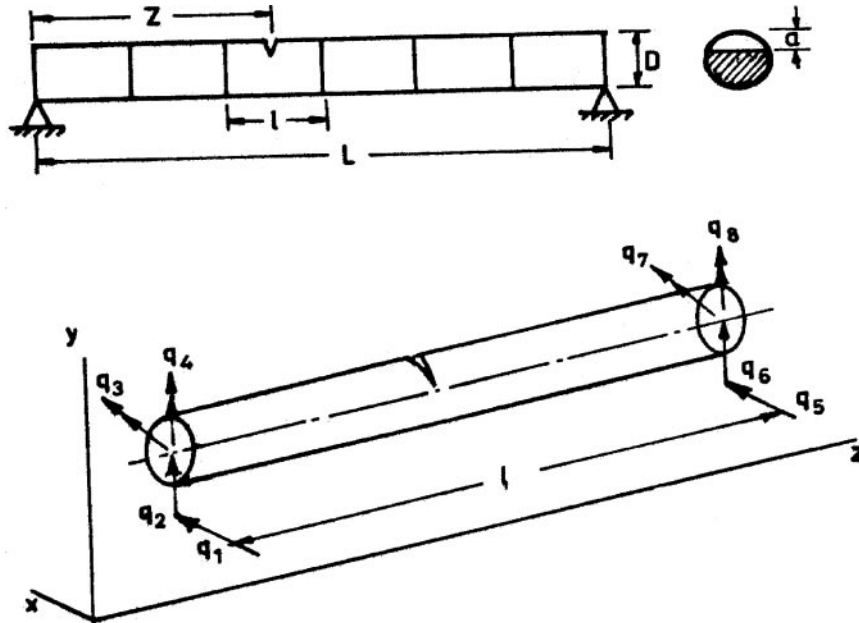


Figure 2 Simply supported shaft with a cracked element.

mass and diametral moments of the rigid disc. The matrix $[D]$ includes the gyroscopic moments, and damping. The stiffness matrix $[K]$ considers the stiffness of the shaft elements and the bearing stiffness. Cracked element stiffness can be included easily, for the cracked rotor analysis. The excitation matrix $\{F\}$ in Equation (14) consists of the unbalance forces due to disc having mass m , eccentricity e and the weight of the disc. The unbalance force components in x and y directions for angular rotation θ are given as,

$$\begin{aligned} F_x &= me\{\ddot{\theta} \sin \theta + \dot{\theta}^2 \cos \theta\}; \\ F_y &= me\{-\ddot{\theta} \cos \theta + \dot{\theta}^2 \sin \theta\}. \end{aligned} \quad (15)$$

4 Crack Modelling

The transverse breathing crack has been considered in the present study. The flexibility matrices of the cracked section as given in Papadopoulos and Dimarogonas [27] are utilized for crack modelling. The flexibility coefficients for an element without crack by neglecting shearing action are given by,

$$C_0 = \begin{bmatrix} l^3/3EI & & & & SYM \\ & 0 & l^3/3EI & & \\ & 0 & -l^2/2EI & l/EI & \\ & l^2/2EI & 0 & 0 & l/EI \end{bmatrix},$$

where EI is the bending stiffness and l is the element length. During the shaft's rotation, the crack opens and closes, (the breathing action of the crack) depending on the rotor deflection [28]. For the large class of machines, the static deflection is much greater than the rotor vibration. With this assumption, the crack is closed when $\phi=0$ and it is fully open when $\phi=\pi$ (see Figure 3). The transverse surface crack on the shaft element introduces considerable local flexibility due to strain energy concentration in the vicinity of the crack tip under load. The additional strain energy due to the crack results in a local flexibility matrix C_c , which will be C_{op}

and C_{HC} for a fully open crack and half-open, half-closed conditions, respectively:

$$C_{op} = \frac{1}{F_0} \begin{bmatrix} \bar{C}_{11}R & & & & SYM \\ & 0 & \bar{C}_{22}R & & \\ & 0 & 0 & \bar{C}_{33}/R & \\ & 0 & 0 & \bar{C}_{43}/R & \bar{C}_{44}/R \end{bmatrix},$$

$$C_{HC} = \frac{1}{2F_0} \begin{bmatrix} \bar{C}_{22}R & & & & SYM \\ & 0 & \bar{C}_{11}R & & \\ & 0 & 0 & \bar{C}_{44}/R & \\ & 0 & 0 & \bar{C}_{34}/R & \bar{C}_{33}/R \end{bmatrix}$$

where $F_0 = \pi ER^2/(1 - \nu^2)$, $R = D/2$ and $\nu = 0.3$. The dimensionless compliance coefficients, \bar{c}_{ij} , are functions of non-dimensional crack depth, $\bar{\alpha}(\alpha/D)$, where α is the crack depth in shaft diameter D (see Figure 2). These compliance coefficients are computed from the derivations discussed in [27]. The total flexibility matrix for the cracked section is given as [28],

$$[C] = [C_0] + [C_c]. \quad (16)$$

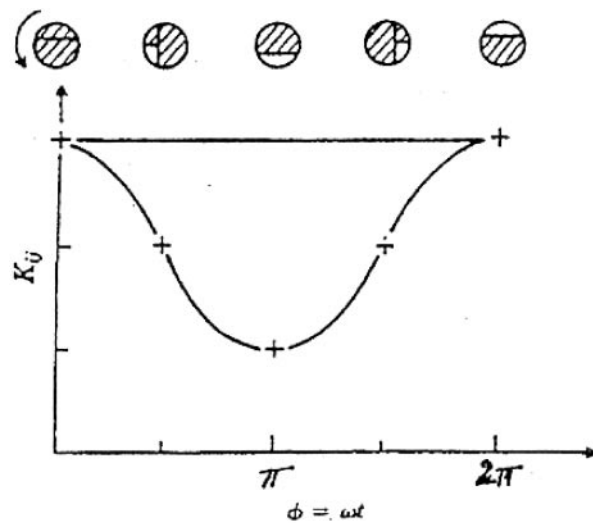


Figure 3 Breathing crack model.

As explained before, C_c will be C_{op} or C_{HC} depends on the breathing position of crack (see Figure 3).

From the equilibrium condition (see Figure 2)

$$(q_1, q_2, \dots, q_8)^T = [T](q_5, \dots, q_8)^T, \quad (17)$$

where the transformation

$$T = \begin{bmatrix} -1 & 0 & 0 & -l & 1 & 0 & 0 & 0 \\ 0 & -1 & l & 0 & 0 & 1 & 0 & 0 \\ 0 & 0 & -1 & 0 & 0 & 0 & 1 & 0 \\ 0 & 0 & 0 & -1 & 0 & 0 & 0 & 1 \end{bmatrix}^T.$$

4.1 Stiffness Matrix

The stiffness matrix of the cracked element is written as [28],

$$[K_c] = [T][C]^{-1}[T]^T \quad (18)$$

When the shaft is cracked, during the rotation the stiffness varies with time, or with angle. The variation may be expressed by a truncated cosine series,

$$[K] = [K_0] + [K_1] \cos \omega t + [K_2] \cos 2\omega t + [K_3] \cos 3\omega t + [K_4] \cos 4\omega t, \quad (19)$$

where $[K_\eta]$, $\eta=0,1,\dots,4$, are fitting coefficient matrices, determined from the known behaviour of the stiffness matrix at certain angular locations [28]. These are obtained from the compliance matrices C_o , C_{op} and C_{HC} together with Equation (18).

5 Continuous Wavelet Transform

Wavelet analysis is similar to Fourier analysis in the sense of breaking of the signal into its constituent parts for analysis. The Fourier transform breaks the signal into a series of sine waves of different frequencies, whereas the wavelet transform breaks the signal into its scaled shifted versions of the mother wavelet. The CWT of $f(t)$ is a time-scale method of signal processing that can be defined as the sum

over all time of the signal multiplied by scaled, shifted versions of the wavelet function $\Psi(t)$. Mathematically,

$$\text{CWT}(s, b) = \frac{1}{\sqrt{|s|}} \int_{-\infty}^{\infty} f(t) \Psi^* \left(\frac{t-b}{s} \right) dt \quad (20)$$

where $\Psi(t)$ denotes the mother wavelet. The parameter s represents the scale index, which is reciprocal of frequency. The parameter b indicates the time shifting (or translation). The CWT provides the time–frequency information of the signal. This means that any non-stationary event can be localized in time unlike Fourier analysis. Additionally, the frequency content of these events can be described for any position on the time axis. This property of CWT has been used in the present study to extract significant characteristics, which are embedded in time domain signal of the cracked rotor passing through its critical speed.

The Morlet mother wavelet [29] with support length of $(-4, 4)$ has been chosen in the present study for all the CWTs. A scale 4 of the CWT is chosen such that the centre frequency of the daughter wavelet in the frequency domain should not coincide with the critical and sub-critical speeds.

6 Results and Discussion

A rotor system with two flexible bearings and two rigid disks as shown in Figure 4, has been considered in the present analysis. The data for the rotor system are given in Table 1. The analysis has been carried out using FEM for flexural vibrations. The eigenvalues are given in Table 2, while the mode shapes are shown in Figure 5. A crack at the mid of the rotor and in the centre of the element 7 (see Figure 4) is considered for the study. When the speed of rotation is changing, the angular displacement can be taken as $\theta(t) = \omega_0 t + 1/2(at^2)$, where ‘a’ is the angular acceleration ($\ddot{\theta}$) of rotor, ‘ ω_0 ’ is the initial angular velocity and a is chosen as 50 rad/s². Houbolt time marching technique is used to model the system in time domain with a time step

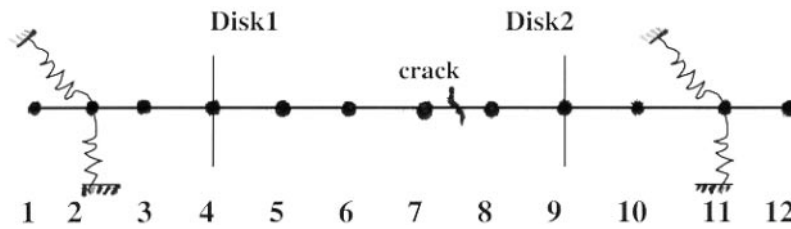


Figure 4 Typical rotor-bearing system considered.

Table 1 Rotor-bearing data.

Length of the rotor (L)	0.780 m	
Shaft		
Diameter (D)	0.02 m	
Density	7850 kg/m ³	
Modulus of elasticity	2.1×10^{11} N/m ²	
Damping ratio	0.01	
Discs		
Masses: m_1, m_2	6.45, 4.27 kg	
Unbalance eccentricity	0.01 mm	
Crack		
Location	6 and 7 element	
Depth (α)	1.4 and 4 mm	
Non-dimensional depth ($\bar{\alpha}(\alpha/D)$)	0.07 and 0.2	
Bearing stiffness (N/m)		
Left bearing stiffness	in horizontal direction	0.105×10^6
	in vertical direction	0.150×10^6
Right bearing Stiffness	in horizontal direction	1.06×10^6
	in vertical direction	1.02×10^6
Acceleration of rotor (a)	50, 100 and 125 rad/s ²	

Table 2 Eigen frequencies of rotor system.

Mode No.	Eigen frequencies (Hz)
1	16.85 (H)
2	28.16 (V)
3	30.38 (H)
4	70.24 (V)
5	71.63 (H)
6	124.76 (V)

of 0.001 s, due to better convergence of results [28]. The time response has been modelled until the system passes 1st the critical speed, which is around 100 rad/s (see Table 2).

In the present study, in the beginning, the vibrations are considered at all the 48 DOF of the model, and this is considered as a reference case. However, normally the vibrations are measured only with few sensors or transducers.

Hence, only for few DOF the measured vibration data are available. Thus the study is done considering less than 48 DOF, such as with 24, 20, ..., 4 DOF. For such less DOF, the vibration data at all the DOF of the rotor are estimated using the modal expansion as explained in Section 2.2. The identification algorithm is searched for crack.

The typical results with crack depths 4, and 1.4 mm are given in the Tables 3 and 4 for 50 rad/s². In all these tables and in subsequent figures showing the results, one point is to be noted. The measured data available at certain DOF means, as explained previously, that only at such number of DOF, the vibration data are available. In this study no experimental data are available, only it is simulated using modal expansion for few DOF cases. In the absence of experimental validations, the simulation results

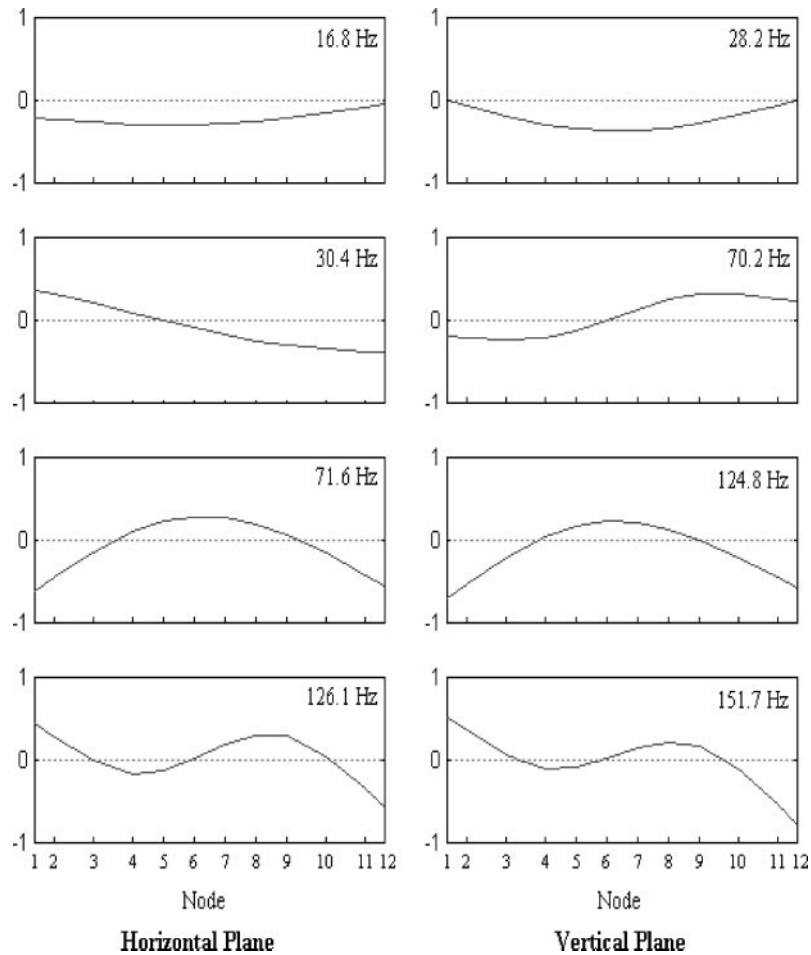


Figure 5 Mode shapes of rotor system.

Table 3 Results of crack identification (crack of depth 4 mm in element No. 7), $a = 50 \text{ rad/s}^2$.

S. No	Measured Data Available at	Estimated Crack Location (Element No.)	Estimated Crack Depth in mm (α)	Probability Measures in %	
				Coherence	Intensity
1	48 DOF reference case	7	4.0	100	25.0
2	Noise Signals	7	3.98	99.89	24.98
3	Modelling error	7	3.92	99.90	25.0
4	Calibration error	7	4.0	99.99	25.0
5	24 DOF	7	2.80	99.96	24.14
6	20 DOF	7	2.62	99.96	18.86
7	8 DOF	7	1.26	99.86	15.00
8	4 DOF	7	1.20	94.78	25.0

are presented with several effects such as noise etc. contaminating the simulations. The simulations were done with the effects of measurement noise; modelling error and calibration error for one crack depth are given in Table 3. The results showed their effects to be low (hence, these

effects are not considered in Tables 4 and 5) thus showing the effectiveness of the identification method/approach. These are discussed in the following paragraphs (refer to Table 3).

Case 1: The time-histories of displacements, velocities and accelerations were exactly measured

Table 4 Results of crack identification (crack of depth 1.4 mm in element No. 7), $a = 50 \text{ rad/s}^2$.

S. No	Measured Data Available at	Estimated Crack Location (Element No.)	Estimated Crack Depth in mm (α)	Probability Measures in %	
				Coherence	Intensity
1	48 DOF reference case	7	1.40	100	25.0
2	24 DOF	7	1.06	99.99	24.24
3	20 DOF	7	0.96	99.99	19.65
4	16 DOF	7	0.46	99.99	15.0
5	4 DOF	7	0.30	99.98	25.0

Table 5 Results of Crack identification (crack of depth 1.4 mm in element No. 7), $a = 100 \text{ rad/s}^2$.

S. No	Measured Data Available at	Estimated Crack Location (Element No.)	Estimated Crack Depth in mm (α)	Probability Measures in %	
				Coherence	Intensity
1	48 DOF reference case	7	1.40	100	25.0
2	24 DOF	7	1.06	99.99	24.23
3	20 DOF	7	0.96	99.99	19.71
4	16 DOF	7	0.46	99.99	15.0
5	4 DOF	7	0.30	99.99	25.0

at all the 48 DOF of the rotor system, so modal expansion was not necessary. The crack depth and location were identified exactly. This case was considered as reference case.

Case 2: In this case all the measuring signals were falsified by band-limited noise. The standard deviation of the disturbances was about 2% of the amplitude of the correct signal. The crack has been identified exactly in element 7 with negligible error in estimating the depth.

Case 3: In this case 5% modelling error has been introduced in both stiffness and mass matrix. In this case also, the crack has been identified exactly in element 7 with negligible error in estimating the depth.

Case 4: In this case calibration errors of 10% in the sensors at both bearings (also at disks separately) were simulated. The crack depth and location were identified exactly.

Cases 5–8: Normally the vibrations are measured only with few sensors or transducers. Hence, only for few DOF the measured vibration data are available. Thus the study is done considering less than 48 DOF, such as with 24, 20, . . . , 4 DOF in Cases 5–8. The modal expansion technique has been used in these cases.

The results show that even for a small crack (1.4 mm or $\bar{\alpha} = 0.07$) and with fewer measured data (less DOF such as 4, 8), the location of the

crack has been identified effectively. The results show that with decrease in measured vibration data (less DOF) the error in estimating the depth has increased. This is expected as the full vibration data of unmeasured locations using the mode shape of undamaged rotor system cannot be accurately estimated from fewer data points. However, the location has been identified successfully. From the practical point of view, if we have a good number of sensors, the depth estimation is not going to be a problem. For fewer DOF, the rotor can be stopped and checked for exact depth of the crack. However, one should not get misled by the depth it has been estimated online and proceed to continue running the rotor. The crack depth should be estimated by considering this error, if to determine when the machine must be removed from service, since stopping the rotor is very expensive and not always practical. However, better expansion techniques or refined modal expansion methods should be incorporated to get better results and to finally implement this scheme in practice.

The identification process is repeated for acceleration of 100 rad/s^2 , the results of which (see Table 5) are almost identical as that of 50 rad/s^2 . Thus even for the higher acceleration, the crack identification is quite effective. The crack identification process using model-based method algorithm with the residual vibrations

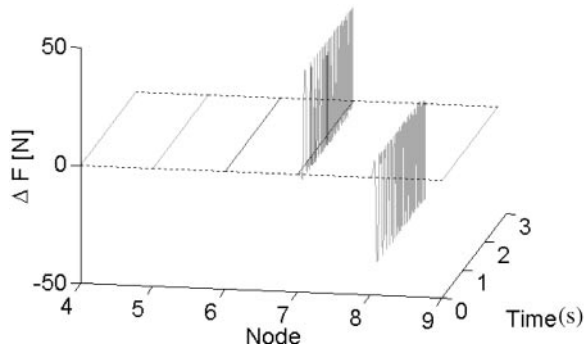


Figure 6 Reference case (48 DOF) : estimated equivalent loads, for crack of depth 4 mm in element 7, $a = 50 \text{ rad/s}^2$.

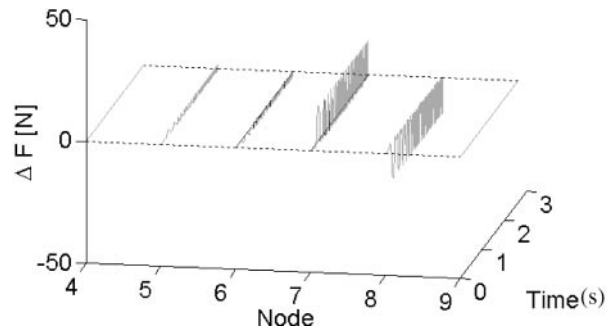


Figure 7 Estimated equivalent loads (24 DOF), for crack of depth 4 mm in element 7, $a = 50 \text{ rad/s}^2$.

estimated the equivalent loads for the reference case (48 DOF) for rotor acceleration of 50 rad/s^2 and are shown in Figure 6. From this figure, it is clear that the equivalent forces are observed only at the nodes 7 and 8, which are the nodes of the cracked element. Hence, this method identified the crack at the exact location and also estimated the depth correctly (20% of the shaft diameter = 4 mm – see Table 3). Further, the crack identification results with fewer measured data (less DOF) are shown in Figures 7 and 8. In all the cases including the case of 4 DOF (see Figure 8(a) and (b)) the equivalent forces are observed dominantly at the nodes 7 and 8 of the cracked element no. 7. That means the crack location has been identified successfully.

The location of the crack has been changed from 7th to 6th. Then also the crack has been identified at the correct location. The details are shown in Figure 9(a) and (b). But, for the

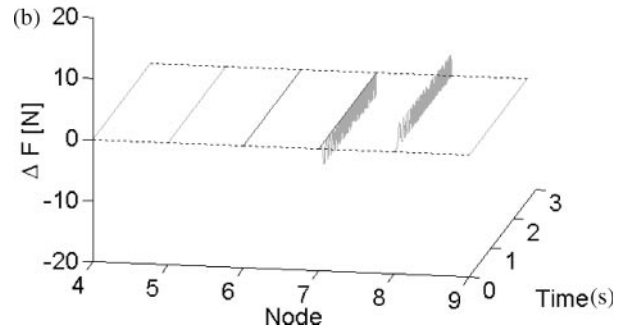
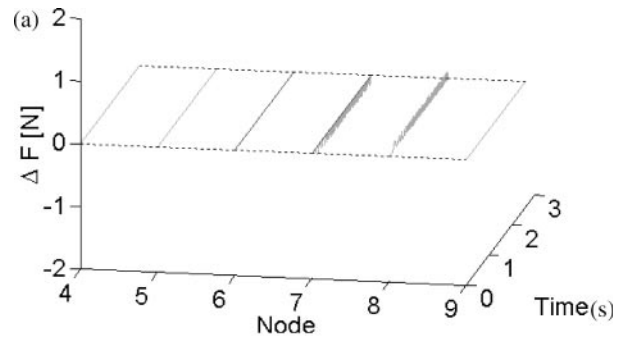


Figure 8 (a) Estimated equivalent loads (4 DOF), crack of depth 1.4 mm in element 7, $a = 50 \text{ rad/s}^2$; (b) estimated equivalent loads (4 DOF), crack of depth 4 mm in element 7, $a = 50 \text{ rad/s}^2$.

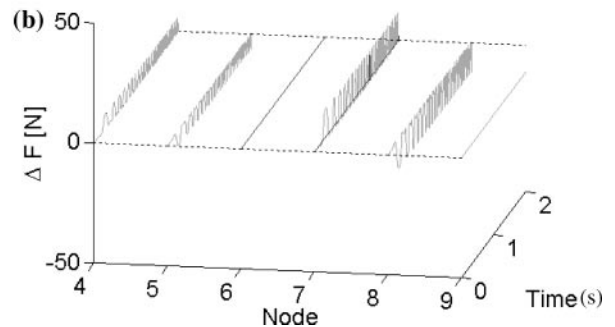
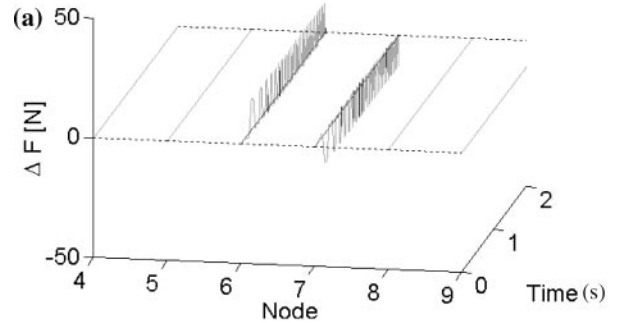


Figure 9 Estimated equivalent loads (20 DOF) for different crack locations, crack depth 4 mm, $a = 50 \text{ rad/s}^2$: (a) Crack in 6th element; (b) crack in 7th element.

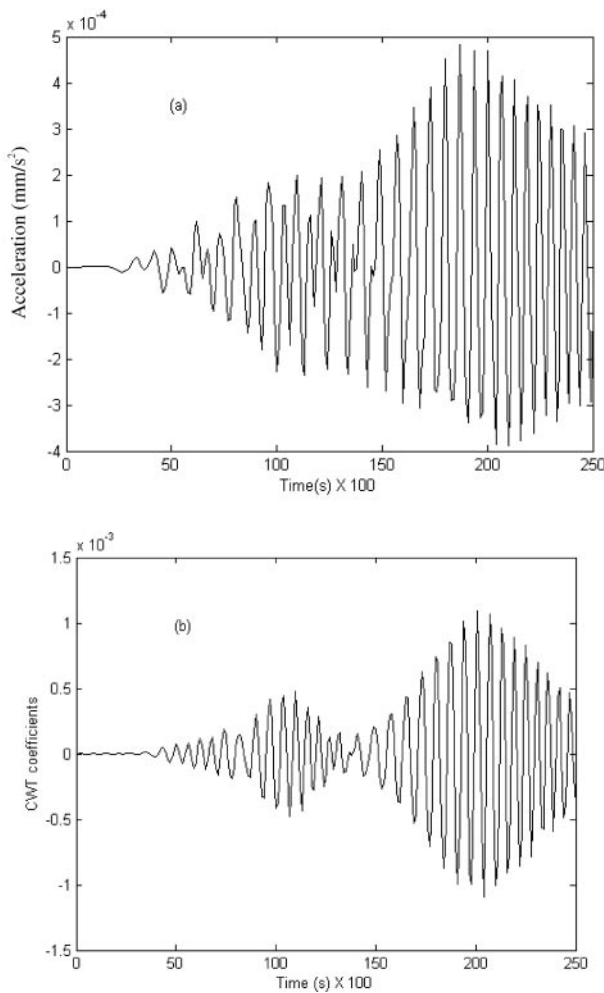


Figure 10 Residual vibrations at disk1, for crack depth 1.4 mm in element 7 (4 DOF), $a = 50 \text{ rad/s}^2$: (a) Time; (b) CWT.

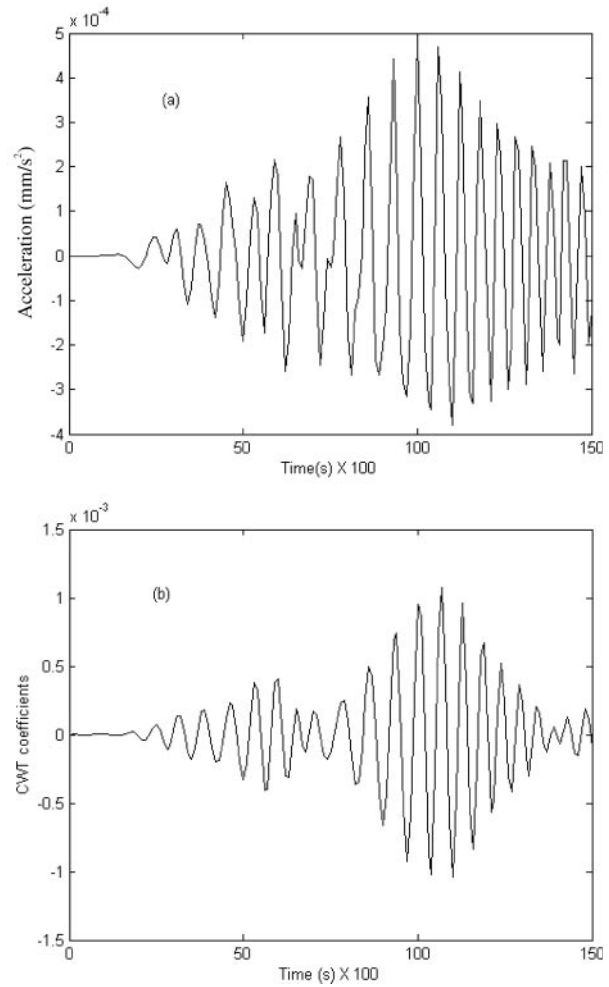


Figure 11 Residual vibrations at disk1, for crack depth 1.4 mm in element 7 (4 DOF), $a = 100 \text{ rad/s}^2$: (a) Time; (b) CWT.

estimation of crack depth, the error has increased with the few measured data, as explained before. However, since the crack has been identified at the correct location, the error in the estimation of crack depth may not be a serious problem. Further, the symptoms of the present fault are found using the wavelet analysis. In the present study continuous wavelet transform (CWT) as explained in Section 5 is used. The details are explained through the following figures.

The model-based technique with modal expansion for the case of 4 DOF, has been applied considering a small crack depth of 1.4 mm in the element 7, for different rotor accelerations. The results are shown in Figures 10–12. In all

these figures, the residual vibrations due to crack, measured at disk1 are shown in both time-response and their wavelet coefficients. Since the rotor is passing the critical speed, the vibrations are non-stationary in nature, hence the CWT of the response has been determined. In Figure 10, a main peak at about 2 s, is observed corresponding to critical speed ($16.85 \text{ Hz} = \text{around } 100 \text{ rad/s}$) when the rotor is accelerated with 50 rad/s^2 . Apart from this, the 1/2 critical at 1s can be observed from Figure 10, which is characteristic of the crack. The sub-harmonic resonant peak is observed even in the time-response (Figure 10(a)), and quite clearly in the wavelet (Figure 10(b)). Also the slight 1/3 critical (at around 0.65 s)

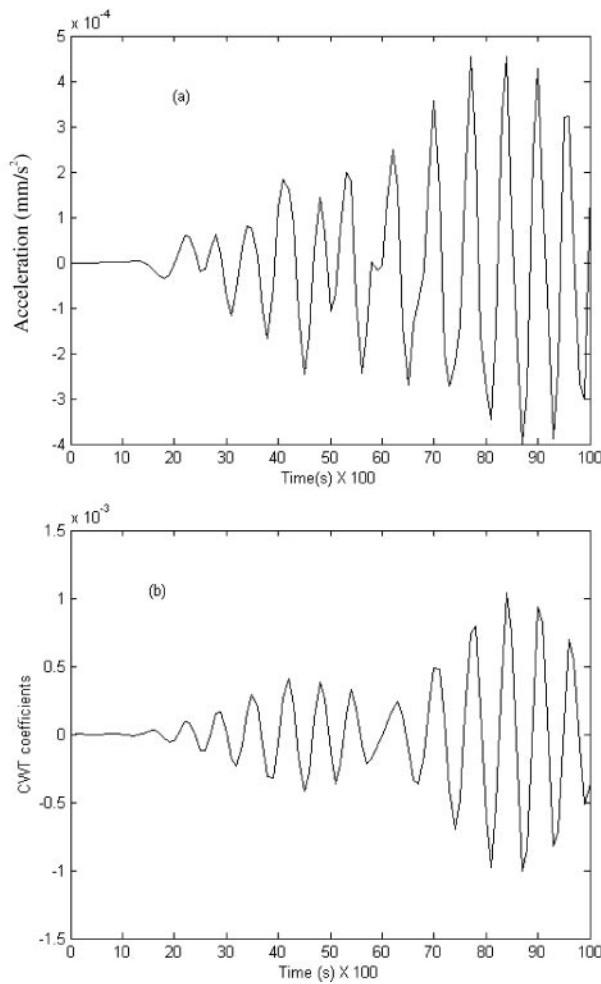


Figure 12 Residual vibrations at disk1, for crack depth 1.4 mm in element 7 (4 DOF), $a = 125 \text{ rad/s}^2$: (a) Time; (b) CWT.

speed can be noticed from the CWT (Figure 10(b)), indicating the presence of a crack.

The CWT is compared with time-response for various rotor accelerations in Figures 10–12. Similar to Figure 10, the crack behaviour for $1/2$ critical are observed in Figures 11 and 12. At low accelerations (Figure 10) the sub-harmonic resonant peaks are clear from the CWT plot and even in the time-response plot because the time taken to pass through the critical and sub-critical speeds is more. However, as the acceleration increases (Figures 11 and 12) the sub-harmonic resonant peaks are embedded in time-response and these can be extracted by using CWT. Thus it is found that CWT is a powerful tool for detecting cracks

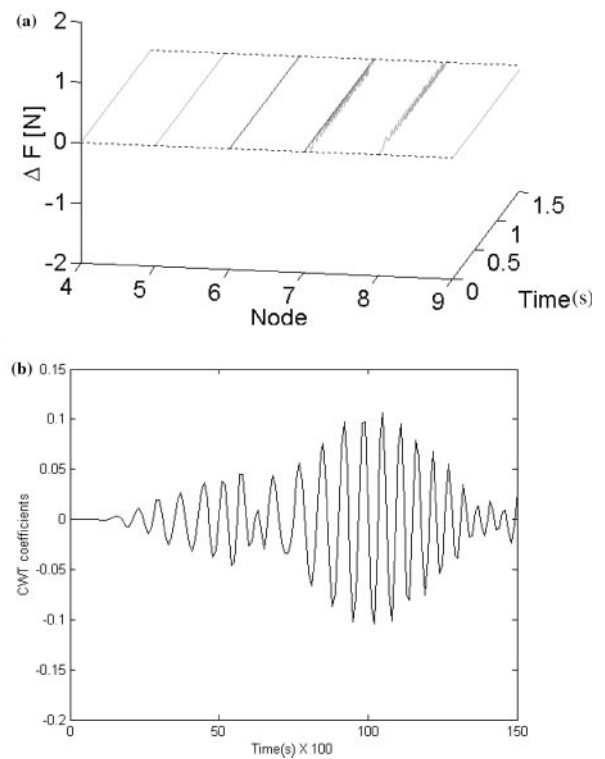


Figure 13 Identification of crack of depth 1.4 mm in element 7 (4 DOF) at rotor acceleration, $a = 100 \text{ rad/s}^2$: (a) Estimated Equivalent loads; (b) CWT of (a).

particularly at high accelerations and low crack depths compared to time responses.

Further, the symptoms of the present fault are found using the CWT of the time-response of estimated equivalent force from the identification (Figure 13). From the Figure 13(b), which shows the CWT of the estimated equivalent force, the sub-harmonic peak, $1/2$ of critical speed is observed clearly. Thus a model-based method together with the wavelet, can be used effectively to identify and monitor the crack in a rotor passing the critical speed.

If the experimental results are available, one can easily use them as measured data and apply the modal expansion to identify the crack effectively, in this case of transient response also. The model-based identification technique with modal expansion has been successfully demonstrated for crack location. For the better estimation of crack depth, one can refine the modal expansion, considering some weighting functions or

some suitable curve fitting functions etc., together with the mode shapes.

7 Conclusion

A complex rotor-bearing system has been modelled using FEM. The model-based identification technique with modal expansion has been successfully demonstrated for different crack locations and depths at different rotor accelerations, passing the critical speed. In addition the advanced signal processing such as the CWT has been used to extract the sub-harmonic features of crack successfully from the time-response. Thus the nature and symptoms of the fault, that is crack, are ascertained.

The effectiveness of the identification process depends to a good extent on the number of measured locations (DOF). However, this is for only to the extent of estimating crack depth.

Acknowledgements

The author would like to thank the financial support of the Alexander von Humboldt Foundation to carry out this research. Also, he would like to thank the support, discussion and facilities provided by Prof. R. Markert and his work group.

References

1. Wauer, J. (1990). Dynamics of cracked rotors: literature survey. *Applied Mechanics Reviews*, 43, 13–17.
2. Gasch, R. (1993). A survey of the dynamic behaviour of a simple rotating shaft with a transverse crack. *J. Sound and Vibration*, 160, 313–332.
3. Dimarogonas, A.D. (1996). Vibration of cracked structures: a state of the art review. *Engg. Fracture Mechanics*, 55, 831–857.
4. Hass, H. (1977). Großschaden durch turbinen- oder Generatorlaufer, entstanden im Berench bis zur Schleuderdrehzahl, *Der Maschinenschaden*, pp. 195–204. 50, Heft 6, In German.
5. Muszynska, A. (1982). Shaft crack detection, Seventh machinery dynamics seminar, Canada.
6. Gasch, R. (1976). Dynamic behaviour of a simple rotor with a cross sectional crack. *I. Mech. Conference, Vibration in Rotating Machinery*, Paper No. C 178/76.
7. Mayes, I.W. and Davies, W.G.R. (1984). Analysis of the response of a multi-rotor-bearing system containing a transverse crack in a rotor. *ASME Journal of Vibration, Acoustics, Stress and Reliability in Design*, 106, 139–145.
8. Inagaki, T., Kanki, H. and Shiraki, K. (1982). Transverse vibrations of a general cracked – Rotor bearing system. *ASME Journal of Mechanical Design*, 104, 345–355.
9. Hamidi, L., Piand, J.B., Pastorel, H., Mansour, W.M. and Massoud, M. (1994). Modal parameters for cracked rotors – Models and comparisons. *J. Sound and Vibrations*, 175, 265–278.
10. Edwards, S., Lees, A.W. and Friswell, M.I. (1998). Fault diagnosis of rotating machinery. *Shock and Vibration Digest*, 30(1), Jan .
11. Seibold, S. and Weinert, K. (1996). A time domain method for the localization of cracks in rotors. *J. Sound and Vibration*, 195(1), 57–73.
12. Bach, H. and Markert, R. (1997). Determination of the fault position in rotors for the example of a transverse crack. In: Fu-Kuo Chang (ed.), *Structural Health Monitoring*, pp. 325–335, Technomic Publ, Lancaster/Basel.
13. Platz, R., Markert, R. and Seidler, M. (2000). Validation of online diagnostics of malfunctions in rotor systems. *Proc. of the 7th Int. Conf. On Vibrations in Rotating Machinery*, pp 581–590, IMech., UK.
14. Markert, R., Platz, R. and Seidler, M. (2000). Model based fault identification in rotor systems by least squares fitting, ISROMAC-8, Honolulu, Hawaii, March 2000.
15. Edwards, S., Lees, A.W. and Friswell, M.I. (2000). Estimating rotor unbalance from a single run-down. *Proc. of the 7th Int. Conf. on Vibrations in Rotating Machinery*, pp 323–334, IMech., UK.
16. Bachschmid, N. and Pennacchi, P. (2000). Model based malfunction identification from bearing measurements. *Proc. of the 7th Int. Conf. on Vibrations in Rotating Machinery*, pp 571–580, IMech., UK.
17. Bachschmid, N. and Dellupi, R. (1996). Model-based diagnosis of rotor systems in power plants – A research funded by the European community. *Proc. of the 6th Int. Conf. on Vibrations in Rotating Machinery*, pp. 50–55, IMech., Oxford, UK.
18. Mayes, I. and Penny, J.E.T. (1998). Model-based diagnostics of faults rotating machines. *Proc. of the 12th Int. Congress on Condition Monitoring and Diagnostic Engineering Management*, pp. 431–440, Sunderland, UK.
19. Plaut, R.H., Andruet, R.H. and Suherman, S. (1994). Behaviour of a cracked rotating shaft during passage through a critical speed. *Journal of Sound and Vibration*, 173, 577–589.

20. Sekhar, A.S. and Prabhu, B.S. (1998). Condition monitoring of cracked rotors through transient response. *Journal of Mechanisms and Machine Theory*, 33(8), 1167–1175.
21. Tong, Zhou, Xu, Jianxue and Sun, Zhengce. (2001). Dynamic analysis and diagnosis of a cracked rotor. *ASME Journal of Vibration and Acoustics*, 123, 539–543.
22. Newland, D.E. (1994). Wavelet analysis of vibration, part I: theory. *ASME Journal of Vibration and Acoustics*, 116(4), 409–416.
23. Newland, D.E. (1994). Wavelet analysis of vibration, part II: Wavelet maps. *ASME Journal of Vibration and Acoustics*, 116(4), 417–425.
24. Staszewski, W.J. (1998). Structural and mechanical damage detection using wavelets. *The Shock and Vibration Digest*, 30(6), 457–472.
25. Prabhakar, S., Sekhar, A.S. and Mohanty, A.R. (2001). Detection and monitoring of cracks in a rotor-bearing system using wavelet transforms. *Journal of the Mechanical Systems and Signal Processing*, 15(2), 447–450.
26. Nelson, H.D. and McVaugh, J.M. (1976). Dynamics of rotor-bearing systems using finite elements. *ASME J Engineering for Industry*, 98, 593–600.
27. Papadopoulos, C.A. and Dimarogonas, A.D. (1987). Coupled longitudinal and bending vibrations of a rotating shaft with an open crack. *J Sound and Vibration*, 117, 81–93.
28. Sekhar, A.S. and Prabhu, B.S. (1994). Transient analysis of a cracked rotor passing through the critical speed. *J Sound and Vibration*, 173, 415–421.
29. Daubechies, I. (1994). Ten lectures on wavelets, CBMS, SIAM, 61, 76.